Equilibrium Chain Exchange Kinetics of Diblock Copolymer Micelles: Tuning and Logarithmic Relaxation

Reidar Lund,*,† Lutz Willner, and Dieter Richter

Institute of Solid State Research, Forschungszentrum Jülich, D-52425 Jülich, Germany

Elena E. Dormidontova

Department of Macromolecular Science and Engineering, Case Western Reserve University, Cleveland, Ohio 44106-7202

ABSTRACT: A systematic study of the equilibrium chain exchange kinetics of a tunable model system for starlike polymeric micelles is presented. The micelles are formed by well-defined highly asymmetrical poly-(ethylene−propylene)−poly(ethylene oxide) (PEP−PEO) diblock copolymers. Mixtures of *N*,*N*-dimethylformamide (DMF) and water are used as selective solvents for PEO. With respect to PEP this solvent mixture allows the interfacial tension, γ, to be tuned over a wide range. The equilibrium chain exchange between these micelles has been investigated using a novel time-resolved small-angle neutron scattering (TR-SANS) technique. The results show that the exchange kinetics is effectively frozen for large interfacial tensions but can be readily tuned to accessible time scales (minutes to hours) by lowering γ. Independent of temperature and concentration, the corresponding relaxation functions show an extremely broad and heterogeneous logarithmical decay over several decades in time. We explicitly show that such broad relaxation cannot be explained by polydispersity or a classical distribution of activation energies. Instead, the logarithmic time dependence points toward a complex relaxation picture where the chains are slowed down due to mutual topological and geometrical interactions. We propose that the behavior stems from constrained core dynamics and correlations between the expulsion probability of a chain and its conformation.

1. Introduction

Polymeric micelles are spontaneously formed by self-assembly when block copolymers are immersed in a selective solvent, i.e., a good solvent for one block but a precipitant for the other. This occurs when the polymer concentration is above a certain threshold concentration known as the critical micelle concentration, cmc, in analogy with traditional low molecular weight surfactant micelles. As a consequence of random stochastic forces, some free chains (concentration, $\phi \approx$ cmc) will remain free in solution and exchange between the micelles in a dynamic equilibrium. For low molecular weight surfactant micelles this exchange kinetics have been extensively studied during the 1970−1980s, yielding a good understanding of their dynamical behavior.[1,2] For polymeric micelles, however, the interest so far has mainly been focused on structural properties.[3,4] Their dynamical behavior, such as the chain exchange between the micelles in equilibrium, remains less understood. According to Halperin and Alexander,[7] the kinetics for diblock copolymers is analogous to surfactant micelles and controlled by the Aniansson and Wall mechanism.[5,6] This mechanism allows only unimers (i.e., single chains) to be inserted or expelled at a given time. Exchange through other mechanisms, such as by micellar splitting (fission) and re-formation (fusion), has been found to be energetically unfavored under equilibrium conditions when the micellar distribution is narrow.[7] Additionally, since the corona of polymeric micelles consists of densely packed chains, entropic repulsion will disfavor any fusion between micelles. This was also demonstrated by Dormidontova[8] in a work on the kinetics of micelle formation where the unimer exchange

mechanism gradually takes over to be the unique mechanism as the equilibrium is approached.

Unfortunately, the exchange kinetics of polymeric micelles in real equilibrium is difficult to assess because perturbations are inevitable in most experimental techniques. A classical strategy used to resolve the kinetics of low molecular weight surfactant micelles is to perform a small-amplitude temperature jump and follow the relaxation to the new equilibrium state.[1,9] However, these methods are of very limited use for polymeric micelles as rather large temperature jumps are generally required for detectable signals which consequently disturb the system far away from equilibrium.[10] On the contrary, the Aniansson and Wall theory, which is the basis of the Halperin and Alexander model, assumes only a small linear perturbation. Another and more suitable way is to employ labeled polymers. This has been done by attaching different fluorescent donors and acceptors on the polymers and follow the quenched intensity as the corresponding micelles are mixed.[13,16] Unfortunately, this method is complicated by the fact that often very bulky chemical labels have to be attached which may alter the physicochemical properties of the system. Moreover, energy transfer might occur through unwanted parallel mechanisms which may complicate the data analysis.[14] In this study we employ a newly developed time-resolved small-angle neutron scattering (TR-SANS) technique.[11] This method is ideally suited for the determination of equilibrium exchange kinetics as only labels involving hydrogen/deuterium (H/D) isotope substitution are required which virtually do not perturb the system. Moreover, as the excess number of chains is directly related to the contrast and thereby given by the observed intensity, the kinetics can be unambiguously determined. Additionally, because SANS offers a spatial resolution in terms of the momentum transfer vector, Q, the structure

† Present address: Donostia International Physics Center, Paseo Manuel de Lardizabal 4, 20018 San Sebastián, Spain.
* Corresponding author. E-mail: reidar_lund@ehu.es.

can be monitored simultaneously. The method will be described in more detail in the Experimental Section.

In comparison with low molecular surfactant micelles, the kinetics of polymeric micelles is generally extremely slow. In fact, in a previous study it was found that for PEP5−PEO15 (numbers denote molecular weight in kg/mol) micelles in water the kinetics is essentially frozen at least on the observed time scale of days.[11] This was also concluded for polybutadiene−PEO block copolymer micelles in aqueous solution by Won et al.[12] Other investigations on block copolymers with polystyrene as the core forming polymer in aqueous solutions have shown that the kinetics occurs on time scales virtually ranging from infinity to hours/minutes depending on the nature of the cosolvent and the temperature.[13] However, here the data analysis is complicated by the fact that the glass transition temperature, T_g, of PS is rather high ($T_g \approx 100-105$ °C). A later study revealed that for similar block copolymers the kinetics can be tuned over a wide time window using several cosolvents and cosurfactants in addition to temperature.[16] In any case the exchange kinetics of polymeric micelles proceed on time scales drastically longer than for ordinary surfactant micelles, which are in the order of the microsecond/millisecond (μs−ms) range.[2] The reason for the slow kinetics has generally been attributed to the strong incompatibility between the insoluble polymer block and the solvent. This behavior can be rationalized in terms of the Halperin and Alexander model, where the activation energy for the chain expulsion is directly proportional to the interfacial tension, γ, and the effective surface area of the insoluble part of a single polymer chain. The expulsion rate constant, k, is then exponentially dependent on γ:

$$k = \frac{1}{\tau_0} f(N_A, N_B) \exp(-E_a/k_b T) \quad (1)$$

with k_b the Boltzmann constant and T the absolute temperature. τ_0 is the characteristic diffusion time, and $f(N_A, N_B)$ is a prefactor that depends on the number of repeat units of the insoluble, N_B, and the soluble, N_A, block. For starlike micelles, $f(N_A, N_B) = N_A^{-9/5} N_B^{-2/25}$. E_a is the activation energy given by

$$E_a = \gamma N_B^{2/3} l_B^2 \quad (2)$$

where l_B is the monomer length of the insoluble block. Hence from this theory, the kinetics can be expected to be tuned on a suitable time scale by changing the interfacial tension.

In this work we present results on the equilibrium exchange kinetics of a tunable model system for starlike micelles using TR-SANS. The system consists of micelles formed by highly asymmetric PEP1−PEO20 block copolymers in solvent mixtures of water and *N,N*-dimethylformamide (DMF). Water and DMF are both selective solvents for PEO but differ strongly in the interfacial tension toward the insoluble PEP block: γ(water) = 46 mN/m and γ(DMF) = 8.6 mN/m. This allows γ to be effectively tuned by varying the composition of the solvent mixtures. In a previous publication the structural properties of this system have been presented in detail.[17] SANS investigations have shown that the micelles are spherical, consisting of a small compact PEP core surrounded by a large extended PEO corona. Detailed model fitting revealed that the density profile of the corona is consistent with what has been proposed for starlike structures, i.e., $n(r) \sim r^{-4/3}$.[18,19] Furthermore, the observed variation of the aggregation number, P, with the interfacial tension follows a scaling law predicted for starlike micelles ($P \sim \gamma^{6/5}$).[19] Recent studies[20,21] have also shown that intermicellar interactions and phase behavior of this system are compatible
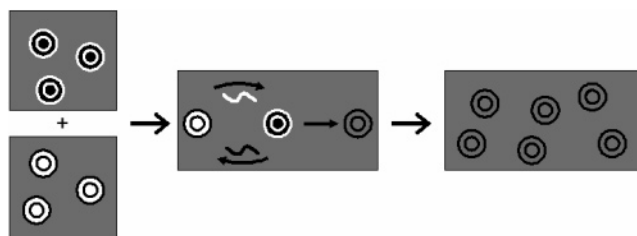
Figure 1. Schematical illustration of the mixing scheme for the TR-SANS technique. Deuterated ("black") and hydrogenated ("white") micelles are mixed at $t = 0$. As the chains exchange the overall scattering length density approaches the solvent ("gray"); the contrast and consequently the scattered intensity vanish.

with the corresponding ultrasoft potential expected for starlike structures.[22] Hence, this system can be used as a tunable model system to study the equilibrium exchange kinetics of starlike micelles. Additionally PEP, which constitutes the core, has the advantage of a very low glass transition temperature ($T_g \approx -56$ °C), in contrast to other previously investigated systems consisting of PS as the core-forming polymer. We therefore expect no complications from any internal glassy dynamics which may complicate the interpretation of the kinetics.

In the following we will show that the kinetics of this system can be tuned on an appropriate time scale with γ, allowing the equilibrium exchange kinetics to be directly observed by TR-SANS. The experimental results reveal a logarithmic time dependence which is interpreted in terms of constrained chain dynamics within the micellar core.

2. Experimental Section

2.1. Time-Resolved SANS Measurements. The equilibrium exchange kinetics of polymeric micelles can be determined using time-resolved SANS under certain contrast conditions.[11] The idea is to mix two micellar populations of different hydrogen/deuterium isotope composition and to observe the decay of the scattered neutron intensity as the chains exchange and the two populations form a homogeneous mixture. A similar idea has been applied to light scattering to study molecular exchange between oil-in-water microemulsions.[23]

Using SANS, this is easily achieved by preparing two block copolymers that are of identical molecular volume and composition but differently labeled, i.e., one fully deuterated (d) and one fully hydrogenated (h). The micelles are then prepared by dissolving each of these block copolymers separately in an isotopic selective solvent mixture that exactly matches the average scattering length density of the two. When the two reservoirs are mixed, this condition corresponds to zero average contrast condition, and as the micellar chains are exchanging, the overall contrast of the micelles is decreasing. Finally, in the completely randomized mixture, the scattered intensity is at minimum where the main contribution arises from the scattering of the individual chain segments within the corona. A conceptual illustration of the idea is given in Figure 1.

The observed SANS intensity is determined by $I(t) \sim (\rho_m - \rho_{Sol})^2$, where ρ_m is the effective scattering length density of the micelle given by the volume fraction of hydrogenated and deuterated chains, f and $1 - f$, respectively: $\rho_m = f\rho_h + (1 - f)\rho_d$, where ρ_h and ρ_d are the scattering length densities of the h and d chains. Since in zero average contrast conditions we have $\rho_{Sol} = \rho_0 = (\rho_h + \rho_d)/2$, we see that the square root of $I(t)$ is linearly proportional to the excess fraction of the h or d chains, i.e., $\sqrt{I(t)} \sim \Delta\rho(t) \sim (f(t) - 1/2)\rho_h + (1/2 - f(t))\rho_d = (f(t) - 1/2)(\rho_h - \rho_d)$. In this way the analysis of the data is straightforward in contrast to other methods. Hence, using this method, the information on the exchange kinetics is unambiguously given by the relaxation function, $R(t)$:

$$R(t) = \left(\frac{I(t) - I_\infty}{I(t=0) - I_\infty}\right)^{1/2} \quad (3)$$

where I_∞ is the scattered intensity of the randomized blend.

Following Halperin and Alexander,[7] the chain exchange kinetics should be simply a first-order chain insertion/expulsion mediated by the solvent. In our experimental setup, we monitor the exchange of d and h chains by effectively measuring the contrast, which is proportional to $(f(t) - \frac{1}{2})$. At the beginning of the experiment when hydrogenated and deuterated micelles are mixed together, the fraction of hydrogenated chains is unity $(f = 1)$ for hydrogenated micelles and 0 for deuterated micelles. At any time t, the fraction of hydrogenated chains in originally 100% hydrogenated micelles is, on average, given by

$$f(t) = f_0(t) + \frac{1}{2}(1 - f_0(t)) = \frac{1}{2}(1 + f_0(t)) \qquad (4)$$

where f_0 is the fraction of original chains that remain in the micelle. The second term in eq 4 is based on the assumption that chains that have been exchanged with free unimers in the solution are equally likely to be deuterated or hydrogenated. This is correct when the time scale of unimer diffusion is much faster than the time scale of chain insertion. As a result, the measured intensity of scattering from originally hydrogenated micelles

$$I_h(t) \sim \frac{1}{4}f_0^2(t)(\rho_h - \rho_d)^2 \qquad (5)$$

is directly proportional to the amount of original chains remaining in the micelle f_0. A similar equation can be obtained for the intensity of scattering for deuterated micelles. The total scattering intensity would be a sum of intensities of scattering from hydrogenated and deuterated micelles, i.e.

$$\sqrt{I(t)} \sim \sqrt{\frac{1}{2}}f_0(t)(\rho_h - \rho_d) \qquad (6)$$

The intensity will tend to zero only when all chains belonging to the originally hydrogenated (or deuterated) micelle have escaped at least once. Thus, our time-dependent scattering intensity directly measures the chain exchange kinetics, which according to Halperin and Alexander is expected to be a first-order kinetic process with a single-exponential behavior:

$$R(t) = \exp(-kt) \qquad (7)$$

The SANS experiments were carried out using the KWS-2 instrument at the cold neutron laboratory of the FRJ2 research reactor at Forschungszentrum Jülich GmbH, Germany. All measurements were performed using standard 2 mm Hellma quartz cells which were mounted in sample holders thermostated by a circulating bath. For the kinetic measurements equal volumes of the micellar solutions were mixed at "$t = 0$" and repeatedly measured in a time increment of every 3 min in the beginning and gradually increasing up to every 30 min at longer times. The samples were thermostated prior to the measurements and mixed in an oven next to the beamline. A typical initial delay was $1-2$ min. The collimation length and sample–detector distance were both 8 m. With a neutron wavelength of 7 Å, a Q range of $4.9 \times 10^{-3}-3.7 \times 10^{-2}$ Å^{-1} was covered. The data reduction and normalization to absolute scale have already been described in an earlier publication.[17] For the kinetic measurements the integral intensity over the whole detector was monitored as a function of time. This was normalized to the incoming neutron flux and compared with the scattering from the reference sample of the randomized blend, I_∞, and the scattering at $t = 0$. The scattering at $t = 0$, $I(t=0)$, was determined from the scattering of the reservoir at low concentrations, $\phi = 0.25\%$, where there is virtually no influence of the structure factor. This is necessary as at higher concentration the structure factor depletes the normalized scattering intensity at low Q, giving rise to a lower absolute integral intensity. After mixing the h and d type micelles under zero average contrast conditions the structure factor cancels.[24] Thus, to properly normalize the relaxation function, the scattered intensity for the two individual micelles was measured at low

Table 1. Molecular Weight Characteristics of the PEP−PEO Block Copolymers

	PEP			PEO		
polymer	M_n	M_w/M_n	N_{PEP}	M_n	M_w/M_n[a]	N_{PEO}
h-PEP1−h-PEO20	1100	1.06	16	21 900	1.04	497
d-PEP1−d-PEO20	1400	1.06	17	23 900	1.04	497

[a] Overall polydispersity of the PEP−PEO block copolymer.

concentrations, normalized to the concentration, and the average used to calculate $I(t=0)$.

2.2. Materials and Sample Preparation. The two block copolymers, h-PEP1−h-PEO20 and d-PEP1−d-PEO20, used in this study were prepared by controlled living anionic polymerization following a two-step procedure as outlined in detail in ref 17. This procedure involves the synthesis of OH-end-functionalized poly-isoprenes which are subsequently saturated with hydrogen or deuterium by means of a conventional Pd/BaSO$_4$ catalyst. The hydroxy-terminated PEP polymers are transferred to a macro-initiator with potassium as counterion to enable the polymerization of ethylene oxide. Special care was exercised such that the blocks made from different isotopes, h-PEP1, d-PEP1 and h-PEO20, d-PEO20, respectively, match in the degree of polymerization. The two block copolymers and corresponding h-PEP1-OH and d-PEP1-OH parent materials were thoroughly characterized by a combination of size exclusion chromatography, ^{1}H NMR, and end-group analysis. Details are also given in ref 17. A summary of the molecular characteristics is listed in Table 1.

The water used in this study was purified by a Millipore apparatus. D$_2$O (Aldrich, 99.8% D), DMF (Aldrich, p.A. quality), and DMF-d_7 (Chemotrade, Leipzig 99.5% D) were used as received without further purifications. A completely randomized blend consisting of 50 vol % of each of the two block copolymers was prepared by dissolving in and freeze-drying from benzene, which is a good solvent for both blocks. This sample serves as the reference for the intensity at "$t \rightarrow \infty$" (final state). Prior to each kinetic run, three samples with virtually identical concentrations were prepared in the respective DMF/water mixtures: one consisting of h-PEP1−h-PEO20, one with d-PEP1−d-PEO20, and one with the blend. The solutions were obtained by dissolving the copolymers in the premixed solvents briefly at 70 °C for ca. 30 min and then shaken until they were completely transparent and no inhomogeneities were visible.

For the kinetic measurements isotopic solvent mixtures of water, D$_2$O, DMF, and DMF-d_7 have to be made such that the resulting scattering length density, ρ_{Sol}, matches the average scattering length density of the two polymers, $\rho_0 = (\rho_h + \rho_d)/2$ (zero average contrast condition). Using $\rho_h = 0.5758 \times 10^{10}$ cm^{-2} and $\rho_d = 7.0348 \times 10^{10}$ cm^{-2} for h-PEP1−h-PEO20 and d-PEP1−d-PEO20, respectively, the average scattering length density, ρ_0, can be calculated to be $\sim 3.80 \times 10^{-10}$ cm^{-2}. The values are calculated using the molecular weight characteristics in Table 1 and the bulk densities of the individual polymer blocks. For h-PEP and d-PEP these values were individually measured as previously reported in ref 17. The bulk density of h-PEO was taken from ref 25, and the density for d-PEO was calculated from d_{h-PEO} assuming equal volumes.

To determine the optimal zero average conditions, the blend and the two reservoirs were measured in a H$_2$O/D$_2$O mixture around the theoretical matching point which should correspond to a D$_2$O mole fraction of $X_{D_2O} = 0.63$. The scattering length densities for H$_2$O and D$_2$O are $\rho = -0.5598 \times 10^{10}$ and 6.2881×10^{10} cm^{-2}, respectively. The results show that the lowest scattering of the blend and the best overlap between the scattering curves from the reservoirs occur at the composition of $X_{D_2O} = 0.58$, corresponding to $\rho_{Sol} \approx 3.47 \times 10^{10}$ cm^{-2}. Consequently, the experimental matching point is slightly smaller than calculated. It is also much smaller than the value calculated on the basis of the apparent solution density of PEO, d_{h-PEO}(solution) ≈ 1.199 g/cm^3,[26] which would imply a larger ρ_0 and an increased D$_2$O fraction $X_{D_2O} = 0.67$ for zero average conditions. The reason for this discrepancy is not fully clear at this point; however, as it is unimportant for the

Table 2. Volume Fractions of PEP–PEO Block Copolymer Solutions, ϕ, and Experimental Scattering Length Densities, ρ_{Sol}, of Representative DMF/Water Solvent Mixtures with DMF Mole Fraction, X_{DMF}

X_{DMF}	ϕ/% h-PEP–h-PEO	ϕ/% d-PEP–d-PEO	ϕ/% blend	$\rho_{Sol}/10^{10}$ cm^{-2}
0	1.016	1.015	1.007	3.5029
0.10	1.002	0.988	0.997	3.4691
0.25	0.990	0.997	0.991	3.4636
0.30	0.994	0.996	0.989	3.4976
0.50	1.034	1.005	1.026	3.5888
0.25[a]	0.249	0.249	0.250	3.4820
0.25[a]	0.506	0.510	0.503	3.4820
0.25[a]	0.982	1.010	1.010	3.4820
0.25[a]	1.982	2.007	2.033	3.4820

[a] Separate measurement series for concentration dependence.
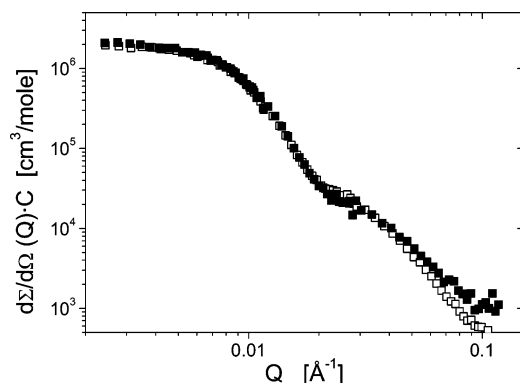
Figure 2. Comparison of the SANS curves in "full contrast" of h-PEP1–h-PEO20 (open symbols) and d-PEP1–d-PEO20 (filled symbols) in D$_2$O and H$_2$O, respectively, at 20 °C and $\phi = 0.25\%$. The data have been normalized by the factor $C = N_A/\Delta\rho^2\phi$, N_A Avogadro number, $\Delta\rho^2$ contrast factor, and ϕ polymer volume fraction.

Table 3. Aggregation Number, P, Core Radius, R_c and Overall Micellar Radius, R_m, of h-PEP1-h-PEO20 and d-PEP1-d-PEO20 in Different DMF/Water Mixtures where X_{DMF} is the Mole Fraction of DMF

X_{DMF}	T [°C]	γ [mN/m]	h-PEP1–h-PEO20			d-PEP1–d-PEO20		
			P	R_m [Å]	R_c [Å][a]	P	R_m [Å]	R_c [Å][a]
0	20	46.0	122	299	39	125	299	41
0.10	20	27.4	74	268	33	78	265	35
0.25	20	21.8	53	226	30	57	236	33
0.30	20	19.7	47	222	29	51	222	31
0.30	42	18.7	46	217	29			
0.30	50	18.0	45	214	29			
0.50	30	14.5	42	196	28	46	213	29

[a] Calculated from P assuming a compact solvent free micellar core. $R_c = (3PV_{PEP}/(4\pi N_A))^{1/3}$, where V_{PEP} is the molar volume of the PEP block and N_A is Avogadro's number.

Figure 3. Scattering curves of a kinetic experiment of h-PEP1–h-PEO20 and d-PEP1–d-PEO20 in D$_2$O/H$_2$O at $\phi = 1\%$: black squares: blend sample ($t \rightarrow \infty$); open squares: arithmetic mean of the two reservoir samples; open circles: scattering curve at $t = 0$; filled stars: the scattering after $t = 24$ h at 70 °C.

results in this work we will not discuss this further. A brief discussion of this issue is given in ref 17.

Consequently, we adjusted the composition of all isotopic solvent mixtures to match the scattering length density of 3.47×10^{10} cm^{-2} using H$_2$O/D$_2$O and DMF/DMF-d_7. The scattering length densities of DMF and DMF-d_7 are 0.6970×10^{10} and 6.3957×10^{10} cm^{-2} at 20 °C, respectively. For details concerning the calculation of the scattering length densities, the reader is referred to ref 17. The concentrations and the scattering length densities of important samples are given in Table 2.
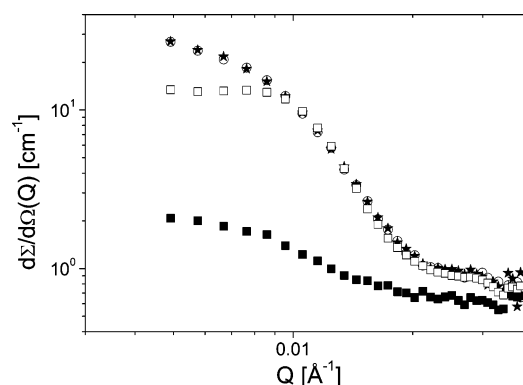
3. Results and Discussion

3.1. Structural Properties of Micelles. An important prerequisite to assess the inherent equilibrium exchange kinetics using the TR-SANS method is that the labeled polymers have approximately the same molecular volume and composition. This is achieved in this work using highly sophisticated controlled anionic polymerization techniques for the preparations of the polymers (Table 1). However, as also the overall micellar properties are of significance, SANS was used to characterize the structure. This has been extensively done and previously published in ref 17. Therefore, the details will not be repeated here. We only give a brief example in Figure 2, demonstrating that the structures of h-PEP1–h-PEO20 and d-PEP1–d-PEO20 micelles in water are indeed similar. The data in Figure 2 have been measured in "full contrast", that is, in D$_2$O for h-PEP1–h-PEO20 and in H$_2$O for d-PEP1–d-PEO20.

The results show that the scattering of the two block copolymer solutions display nearly identical forward scattering and shape. Hence, the overall structural properties of the formed micelles are very similar for both polymers. We further note

that the scattering pattern is very diffuse without any pronounced minima or maxima. As was shown in ref 17, this is not a consequence of large polydispersities but arises from the starlike density profile of the corona which is diffuse and strongly fluctuating.

The micellar parameters were determined by fitting the scattering data to a core–shell model as previously reported in ref 17. Some selected data together with the corresponding interfacial tensions are given for several representative solvent mixtures in Table 3.

3.2. Tuning of Exchange Kinetics. The scattering curves of a kinetic experiment of h-PEP1–h-PEO20 and d-PEP1–d-PEO20 in D$_2$O/H$_2$O are depicted in Figure 3. The figure includes the data from the blend sample of the two polymers representing the completely randomized mixture. The data for the reservoir is the arithmetic mean of the scattering of the two individual reservoirs of h-PEP1–h-PEO20 and d-PEP1–d-PEO20.
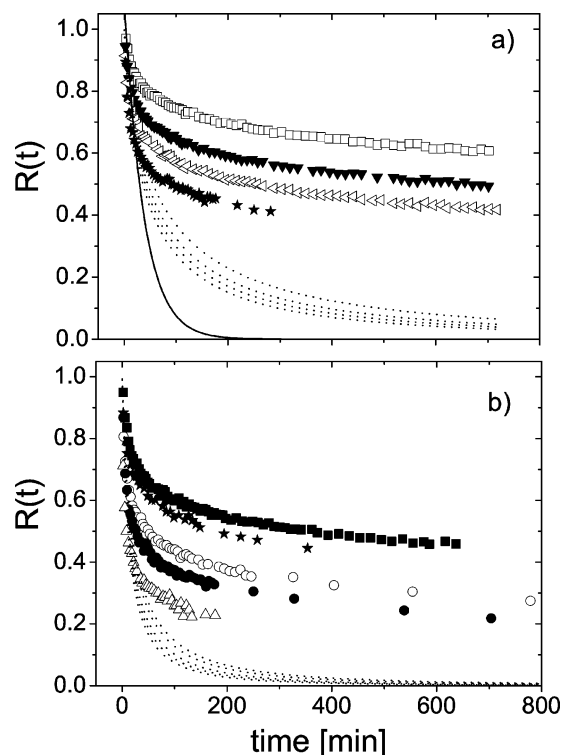
We observe that the intensity at low Q of the mixture is significantly higher than for the scattering from the reservoirs. This is a natural result of the zero average contrast condition where the structure factor influence cancels when two differently labeled but otherwise identical entities are mixed.[24] However, more interesting in this context is that the scattering intensity of the mixture remains unchanged even after heating to 70 °C over a long time. Consequently, it can be deduced that no chain exchange occurs between the micelles in water, and therefore, the system can be regarded as kinetically frozen—at least on the presently observed time scale. Frozen micelles were also found for PEP5–PEO15[11] in water. However, here the molecular weight of the insoluble block was significantly larger, and
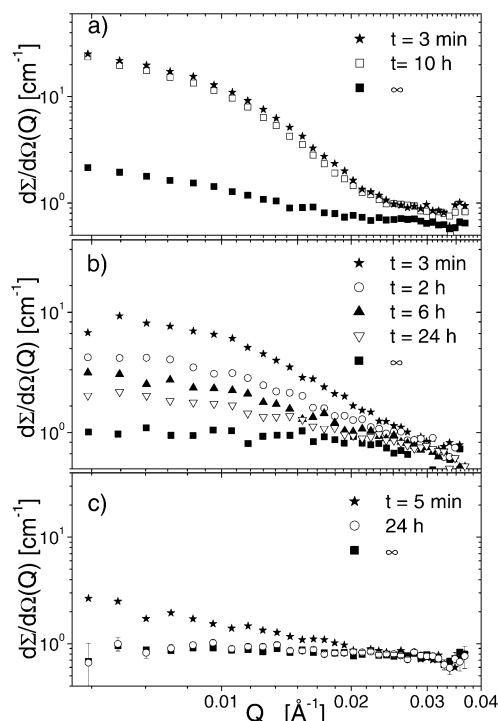
Figure 4. Time evolution of the scattering curves of mixtures of h-PEP1−h-PEO20 and d-PEP1−d-PEO20 in several DMF/water mixtures at $\phi = 1\%$: (a) $X_{DMF} = 0.1$ ($\gamma = 27.4$ mN/m) at 70 °C; (b) $X_{DMF} = 0.3$ ($\gamma = 19.7$ mN/m) at 50 °C, and (c) $X_{DMF} = 0.5$ ($\gamma = 14.5$ mN/m) at 30 °C.
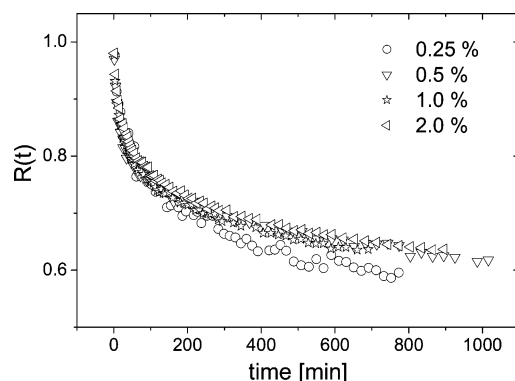

Figure 5. Relaxation kinetics of the PEP1−PEO20/DMF/water system at $\phi = 1\%$ for two solvent compositions at different temperatures: (a) $X_{DMF} = 0.25$. From top to bottom: $T = 47$, 55, 60, and 65 °C. (b) $X_{DMF} = 0.3$. From top to bottom $T = 42$, 47, 55, 60, and 65 °C. The solid line in (a) displays an example of a single exponential predicted by Halperin and Alexander. Dotted lines display simulated curves taking into account the polydispersity of the insoluble PEP block (cf. eqs 8 and 9).

thus a much higher activation energy is expected (cf. eq 2). Nevertheless, the results show that even for the present system when the volume of the insoluble PEP block is reduced by a factor of 5, no exchange occurs. This must be attributed to a large incompatibility between hydrocarbons, such as PEP, and water. This incompatibility is reflected in a large interfacial tension between the polymer and water. For the current system this was quantified by a direct determination of γ using a Pendant Drop instrument.[17] For a PEP homopolymer with the same molecular weight, the interfacial tension was determined to be $\gamma = 46$ mN/m. Thus, recalling eq 2, γ must be lowered in order to observe any exchange. For the PEP−PEO system this can easily be achieved by adding DMF as a cosolvent. Previous studies have shown that γ can be tuned in this way while simultaneously preserving good solvent conditions for PEO.[17]

The influence of addition of DMF on the kinetics is presented in Figure 4. Here the time evolution of the scattering curves of the micellar solutions of PEP1−PEO20 are shown for several DMF/water compositions (mole fraction: X_{DMF}). The data reveal that DMF has a significant effect on the exchange rates. For the mixture containing only a small amount of DMF, $X_{DMF} = 0.1$, virtually no chain exchange can be detected (Figure 4a). At higher DMF fractions progressively faster kinetics can be observed. In terms of the interfacial tension, significant exchange occurs only when γ is lowered to $\gamma = 21.8$ mN/m for $X_{DMF} = 0.25$. Further lowering γ to 19.7 mN/m by adding DMF to $X_{DMF} = 0.30$ achieves an optimal time scale for the applied TR-SANS technique. This can be seen in Figure 4b, where the total intensity of the scattering gradually decreases as a function of time. The data also demonstrate that the overall shape of the scattering curves does not change with time, and in particular no higher order associations such as micellar clustering can be observed at any time. Further increasing the DMF fraction up to $X_{DMF} = 0.5$, which corresponds to $\gamma \approx 14.5$ mN/m, shows

that the intensity has strongly decayed after only 5 min (Figure 4c). Consequently, the kinetics cannot be properly resolved using this technique. It should be pointed out that for this mixture the scattering pattern coincides with the premixed blend within 24 h, demonstrating that the reference state is indeed reached. In the other cases the reference scattering is only reached after an unobservable long time (presumably weeks−months). In the following we will concentrate on systems with 25 and 30 mol % DMF where the kinetics can be most easily followed with TR-SANS.

3.3. Exchange Kinetics. The relaxation curves of the TR-SANS experiment of PEP1−PEO20 in water/DMF with $X_{DMF} = 0.25$ and 0.3 at different temperatures are displayed in Figure 5.

From the data we observe the general trend that the kinetics is fast in the beginning and slows down considerably at long times and is not fully relaxed, even not at times up to 12 h. The kinetics is significantly faster at elevated temperatures; however, a slowdown at long times is still prominent. Comparing with the single-exponential decay predicted by Halperin and Alexander (eq 7), we find no agreement. Only in the very beginning the single-exponential decay coincides with the experimental data. To obtain further insight into the kinetic mechanisms, the polymer concentration was varied from $\phi = 0.25$ to 2% for the system with $X_{DMF} = 0.25$. The results are shown in Figure 6.

The data nicely reveal overlap in the whole time range, except possibly for the lowest concentration ($\phi = 0.25\%$) at long times. However, here the data suffer from poor statistics since the intensity is very low. Therefore, these small deviations can most likely be attributed to the lack of experimental precision under

Figure 6. Relaxation kinetics of the PEP1−PEO20/DMF/water, X_{DMF} = 0.25, system at different polymer concentrations at T = 50 °C.

these conditions. Hence, it can be concluded that the exchange rate does not depend on the micellar concentration, at least not in the studied concentration range which is in the dilute regime ($\phi < \phi^* \approx 4-5\%$[27]). This demonstrates that the kinetics is unimolecular in nature and is essentially determined by the expulsion rate. It is also consistent with the fact that diffusion between micelles does not play any role in the overall rate. This can be further justified by the fact that the diffusion time between the micelles can be estimated to be on the order of microseconds,[28] thus dramatically faster than the time scale of the process here: minutes−hours. Therefore, in the following it can be safely assumed that the kinetics is rate limited by the expulsion time as this is much slower than the insertion process of unimers into the micelles in agreement with expectations in theoretical works.[8,19] According to Halperin and Alexander, for monodisperse polymers, the expulsion rate constant should be given by a single activation energy as described by eqs 1 and 2. As this is obviously in contradiction with the data, we need to consider several or perhaps a distribution of rate constants.

Similar slow and heterogeneous kinetics have been observed for several other systems using fluorescence quenching spectroscopy. PS−PEO block copolymers have been studied in methanol/water mixtures by Wang et al.,[13] poly(styrene)−poly-(isoprene) (PS−PI) in heptane and 1,4-dioxane by Procházka et al.,[14] and poly(styrene)−poly(2-cinnamoylethyl methacrylate) in THF/cyclopentane mixtures by Underhill et al.[15] Here, the relaxation curves were, with varying fit quality, analyzed with a double-exponential decay. This yielded characteristic rate constants well separated in time by 1 or 2 orders of magnitude. This approach was also to a good approximation found to describe the relaxation curves of the PEP5−PEO15/DMF system measured by TR-SANS, as discussed in a previous publication.[11] However, as there is no explanation for an apparent bimodal relaxation and no exclusive fits have been presented in previous works, it is likely that the double exponential is more an approximation to a continuous distribution. Trial fits using such a sum of two exponentials also did not produce any satisfactorily results apart from the first part of the relaxation. Therefore, it is more reasonable to assume a distribution function of relaxation rates.

Parallel Relaxation Scenario: Distribution Functions. It is likely that the broadening of the relaxation may be, to a certain degree, caused by the polydispersity of the block copolymer chains. For the expulsion rate, the polydispersity of the core forming block is most critical as the rate constant is exponentially dependent on the activation energy which is directly related to the molecular weight, cf. Equations 1 and 2. In the present case the polydispersity of the PEP block is very low, $M_w/M_n \leq$ 1.06. Fortunately, the effect of the spread of the block lengths

can easily be taken into account by averaging the H−A single-exponential relaxation over the chain length distribution, $P(N_B)$. It is well-known that for polymers produced by controlled anionic polymerization techniques $P(N_B)$ is given by the Poisson distribution:

$$P(N_B) = \frac{(\langle N_B \rangle - 1)^{N_B - 1} \exp(-(\langle N_B \rangle - 1))}{\Gamma(N_B)} \quad (8)$$

where $\Gamma(x)$ is the gamma function replacing the normal faculty function for continuous variables. The resulting relaxation function can thus be calculated using

$$R(t) = \int_1^\infty P(N_B) \exp(-kt)\, dN_B \quad (9)$$

where k is given by eqs 1 and 2.

The results from this analysis are already shown in Figure 5 as dotted lines. Here only τ_0 has been fitted from the initial decay while all other parameters characterizing the distribution ($\langle N_B \rangle = 16$) and activation energy ($\gamma = 21.8$ mN/m and 19.7 mN/m for $X_{DMF} = 0.25$ and 0.3 respectively, and $l_B \approx 5.1$ Å) have been independently determined by other methods. As clearly demonstrated in the figure, the agreement with the data is slightly improved but is still very poor—the experimental data exhibit a much broader decay than what would arise from polydispersity effects alone. The same results were obtained if instead a general Gaussian distribution was used, and the mean activation energy and its standard deviation were calculated from the Poisson distribution ($\langle E_a \rangle = \langle N_B^{2/3} \rangle l_B^2 \gamma$ and σ_{E_a} and $\sigma_{E_a} = \sqrt{\langle N_B^{4/3} \rangle - \langle N_B^{2/3} \rangle^2} l_B^2 \gamma$). Hence, we can rule out that the inherent distribution of chain lengths of the block copolymers can be responsible for the broad relaxation pattern.

Alternatively, one can assume that the PEP block is not able to adopt a complete compact spherical conformation, owing to the statistics of a small number of segments. This would lead to a different scaling exponent of the activation energy, i.e., $E_a \sim N_B^x$ where $x = 2/3$ in the picture of Halperin and Alexander and $2/3 < x \leq 1$ for globules with more elongated shapes. Even though it seems unlikely to consider large deviations from a spherical shape for PEP in exceptionally bad solvents like DMF/water, such a scenario would lead to an amplification of polydispersity effects. To test this approach, we performed similar calculations using the Poisson distribution but this time letting the scaling factor x to vary. This approach leads to a better description; however, the data could not be fitted satisfactorily for any x, and even for $x = 1$ the temperature dependence of the fitted curves was drastically weaker than found experimentally.

Further broadening of the relaxation can potentially be caused by other factors such as a distribution of micellar sizes and/or the existence of other kinetic mechanisms such as fusion/fission or concerted chain insertion. Other effects such as isotope effects may also potentially play a role. However, as shown above in section 3.1, the micelles are well-defined and the micellar properties of the respective micelles (hydrogenated and deuterated) are the same within 10% (see examples in Figure 2 and in Table 3). In this context the effect of a distribution of micellar sizes will predominantly affect the diffusion time out of the micellar core. However, considering free diffusion, this time will scale as $t \sim P^{2/3}$, and thus one would only expect a very weak broadening by this effect.

Isotope effects can be ruled out for this system. The interfacial tensions of the precursor polymers, h-PEP-OH and d-PEP-OH,

toward water were found to be identical,[29] which is also reflected in the very similar structure of the two types of micelles.

Parallel mechanisms have been proposed as a tentative explanation in other studies where similar slow relaxation kinetics has been observed.[13] Here a distribution of relaxation rates is attributed to parallel mechanisms such as chain transfer by micellar collisions. These mechanisms were also proposed in a Monte Carlo simulation[38] and found to be responsible for a broadening of the relaxation. However, in this experiment where the net decay of contrast is observed, all mechanisms would be independent and occur in parallel with the unimer exchange mechanism. In other words, the total exchange rate constant would be given by the sum of the individual rates with the fastest one determining. Also as observed in Figure 4, the scattering curves have similar shapes at all times during the kinetic processes, indicating that the structure does not vary during the course of the exchange process. Moreover, since the relaxation rates for the current system are found to be concentration independent (see Figure 6), fusion and fission as a parallel mechanism cannot be important. However, we cannot exclude the existence of parallel processes in general, but in any case they cannot be responsible for the broad relaxation behavior in time.

Nevertheless, generally speaking, all factors that would independently contribute to the relaxation can be taken into account by considering a classical distribution function. The most general approach for random independent processes is to assume a Gaussian distribution of activation energies. In terms of rate constants this would be expected to give rise to a log−normal distribution of k, which takes the form

$$R(t) = \int_{-\infty}^{\infty} g(\ln k) \exp(-kt) \, d \ln k \quad (10)$$

where $g(\ln k)$ is the log−normal distribution function given by

$$g(\ln k) = \frac{1}{\sqrt{2\pi}\sigma_{\ln k}} \exp\left(-\frac{(\ln k - \langle \ln k \rangle)^2}{2\sigma_{\ln k}^2}\right) \quad (11)$$

with $\langle \ln k \rangle$ as the mean of the natural logarithm of the rate constant and $\sigma_{\ln k}$ the log−normal width of the distribution. A trial fit using this approach yielded excellent agreements; however, the parameters turned out to be ill defined. To stabilize the fits, the distribution was reexpressed more physically in terms of the parameters from the general Arrhenius relation

$$k = \frac{1}{\tau_0'} \exp(-E_a/RT) \quad (12)$$

where τ_0' is the characteristic "attempt time" to escape the potential well. Then again assuming a Gaussian distribution of activation energies, $g(\ln k)$ can be expressed as

$$g(\ln k) = \frac{RT}{\sqrt{2\pi}\sigma_{E_a}} \exp\left(-\frac{(-RT\ln(k\,\tau_0') - \langle E_a \rangle)^2}{2\sigma_{E_a}^2}\right) \quad (13)$$

where σ_{E_a} is the width of the distribution in units of energy and $\langle E_a \rangle$ the mean activation energy. To test this approach, the data of PEP1−PEO20 in 25 mol % DMF were fitted simultaneously for all temperatures using eq 13 together with eq 10 with $\langle E_a \rangle$, τ_0', and σ_{E_a} as free parameters. Using this approach, excellent fits were obtained but the parameters are unphysical: $\langle E_a \rangle = 165 \pm 1.7$ kJ/mol, $\sigma_{E_a} = 17.6 \pm 0.2$ kJ/mol, and "attempt time" $\tau_0' = (1.7 \pm 0.6) \times 10^{-23}$ s. Similar values were also obtained when the data sets were fitted individually, allowing σ_{E_a} to be
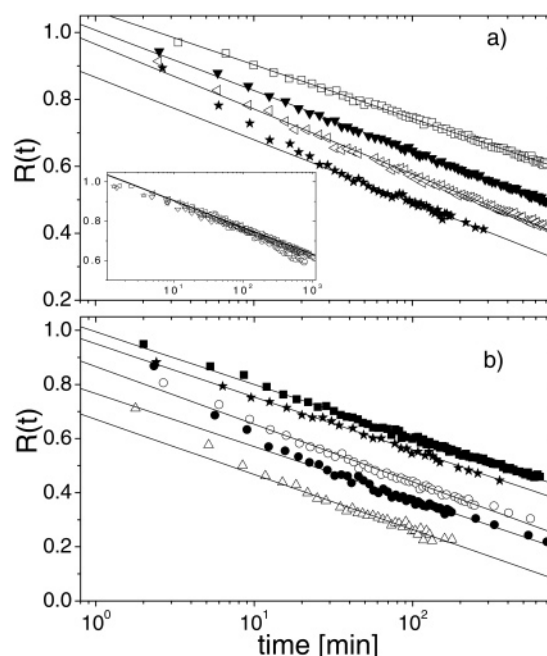
Figure 7. Logarithmic relaxation kinetics. Data of Figure 4 on a logarithmic time scale. Solid lines display linear fits. PEP1−PEO20 in DMF/water solvent mixtures with (a) $X_{DMF} = 0.25$ and (b) $X_{DMF} = 0.30$. The inset plot shows the concentration-dependent data.

temperature dependent. First, the mean activation energy is very large. Indeed, compared with the calculated activation energy from the theory of Halperin and Alexander, $E_a = 21.6$ kJ/mol; this is almost 1 order of magnitude higher. For comparison, the dissociation energy for a carbon−carbon (C−C) covalent bond is ∼347 kJ/mol. Second, the characteristic attempt time, τ_0' of the order of 10^{-23} s, is unphysically low and completely out of any soft-matter frame. In contrast, from the polymer dynamics we would expect the longest Rouse time for PEP to be of the order of 10^{-6} s in this temperature range.[30] Thus, we can conclude that the use of a Gaussian distribution for the activation energies is clearly unapplicable in this context.

Similarly, using a stretched exponential, a general distribution function can be assumed:

$$R(t) = \exp(-(kt)^\beta) \quad (14)$$

where β is the stretching exponent which takes values between 0 and 1. However, this approach did not give satisfactorily fits as the parameters were not well-defined and β approached unreasonable low values ($\beta < 0.2$).

It is also interesting to note that the apparent extremely large activation energy from the free fits of the Gaussian distribution reflect an unusually strong temperature dependence. This can already be seen directly in Figure 5 where the relaxation curves have a pronounced temperature dependence even for small temperature increments of around 5 °C. This strong temperature effect may indicate that the expulsion process is more complicated than a simple activated diffusion process pictured by Halperin and Alexander.

Serial Relaxation Scenario: Logarithmic Time Dependence. When the data are plotted on a logarithmic time scale, straight lines are observed, demonstrating a logarithmic relaxation. This is shown in Figure 7.

$$R(t) \sim -\ln t \quad (15)$$

Such a time dependence indicates an extremely broad continuous distribution that extends over several decades. In

fact, a logarithmic relaxation implies that no inherent natural mean time constant exist. However, there must be a minimal and maximal time as eq 15 will diverge for both $t = 0$ and $t \rightarrow \infty$. This can be avoided using the integral exponential function, $E(x)$,[31] which will approximately give a logarithmic decay between the cutoff rates, k_{min} and k_{max}:[32,41]

$$R(t) = \frac{1}{\ln(k_{max}/k_{min})}(E(k_{min}t) - E(k_{max}t)) \qquad (16)$$

A careful look on the data in Figure 7 reveals that the data do not show deviations that would alow an unambiguous determination of these cutoff rates. For determining k_{max} accurately, more data in the beginning are needed, but as the mixing process of the reservoirs requires a finite time, this is not feasible with the currently applied technique. However, using eq 16, a maximal initial rate constant can be estimated, yielding τ_{min} of the order of minutes. Assuming that $k_{max} = 1/\tau_{min}$ corresponds to the unperturbed rate constant of Halperin and Alexander, the initial time in the system can be estimated from eqs 1 and 2, assuming that the scaling prefactor is of the order of unity. After inserting the relevant parameters, we obtain τ_0 of the order of 10^{-6} s, which is now of the right order of magnitude corresponding to a typical Rouse time of the PEP chains.[30] Thus, contrary to the use of a Gaussian distribution, this description of the data gives reasonable values for the time scales. On the other hand, at long times (up to >12 h) no significant deviations are detectable, and thus no k_{min} can be determined.

The central question is what leads to this apparent broad distribution of relaxation times and the logarithmic time dependence. A logarithmic time dependence has been observed for several complex systems such as in glassy systems,[33] internal dynamics of DNA,[36] kinetics of protein folding,[34,37] and friction experiments.[35] Generally such a relaxation has been assigned to either glassy dynamics with a broad distribution of activation energies[33] or "hierarchical constrained dynamics".[32,37]

In the present case we do not expect any influence of glassy dynamics for the exchange kinetics as T_g of PEP is very low (-56 °C), i.e., much below the measuring temperatures. On the other hand, we are considering global dynamics or, more precisely, the self-diffusion out of the micellar core. Thus, even though one would expect similar local segmental dynamics for chains in a micellar or bulk state, the effective center of mass diffusion may be very different for chains packed in the confinement of a micellar core. Indications of such behavior have been observed for block copolymer melts having a spherical bcc structure, where the self-diffusion of chains systematically slows down and becomes increasingly heterogeneous as the effective interaction parameter χN increases below the order−disorder transition (ODT).[42−44] Since the PEP−PEO system considered here is far above the cmc, we deal with a well-segregated system, and the results can thus be compared with these block copolymer melts when $T \ll$ ODT. A characteristic feature below the ODT is a broad distribution of diffusion times where the relaxation curves can be described by a broad log−normal distribution[42,43] or by a stretched exponential with β parameters as low as 0.25.[44] Thus, comparing with our current micellar system, we see similarities suggesting that the internal dynamics, and consequently the expulsion processes is significantly slowed down due to the segregation and confinement of the chains.

As pointed out by Palmer et al., heterogeneous relaxation behavior can also be caused by strongly coupled dynamics.[39] Here the dynamics is slowed down because the particles are mutually coupled and are forced to relax sequentially instead
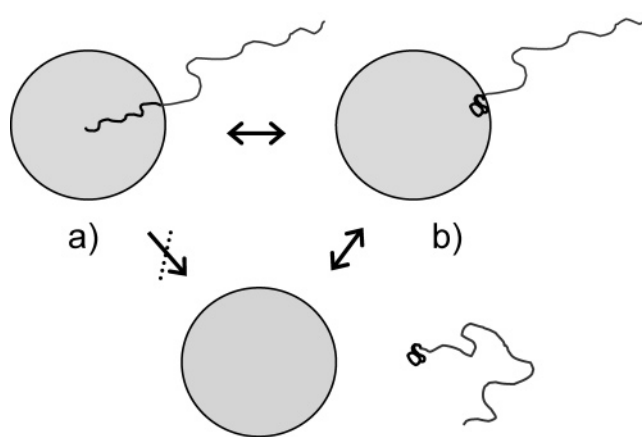
Figure 8. Conceptual scenario for the expulsion of chains from micellar cores. The two upper figures display the extreme conformations possible inside the micellar core: stretched chain (a) and compact chain (b) near the interface. The transition rate between the conformations is slow and rate determining. Only if the sufficiently compact conformation b is achieved, the chain can escape the core as illustrated with the lower figure.

of in parallel. Recent works on this kind of "hierarchical constrained dynamics" demonstrate that such correlations may give rise to a logarithmic time dependence.[32] On the basis of these findings, it is tempting to speculate that similar correlations may be effective for the exchange kinetics of the current micellar system. Since it is well-known that low molecular weight surfactant micelles exchange with a well-defined expulsion rate,[2] the distribution over several decades for the block copolymer micelles must be related to effects arising from its polymeric nature. It should be pointed out that the core-forming PEP blocks are relatively short (16 repeat units corresponding to 64 carbons in the backbone). However, as seen in previous NMR studies, the influence of the confinement on the chain dynamics is strong even for comparable low molecular weight PEO chains and found to be essentially independent of molecular weight.[40] A logarithmical time dependence has also recently been observed for two further micellar systems consisting of symmetric PS−PB block copolymers in a selective solvents for either PB or PS, of which the molecular weights are much larger ($M_{PB} = M_{PS} \approx 10\,000$).[41] Hence, the peculiar exchange kinetics seem to be a general phenomenon characteristic for polymeric micelles.

We hypothesize that the broadening in time is caused by the inherent heterogeneous behavior of polymer chains due to the distribution of chain conformations in the micellar cores. As the chains experience an increasing repulsion as they approach the interface and the contact with the solvent increases, the probability for expulsion is likely to be coupled with the conformational state of the polymer chain.

For polymeric micelles we postulate that the conformation of the chain and its probability to escape the core is intimately correlated. Only when the chain has a sufficiently compact conformation near the interface the probability to be expelled is comparable to the probability to stay in the core. This also implies that chains with this conformation have a greater probability for exchange and consequently will exchange many times (with the same or another micelle) before the more deeply buried chains have time to reorganize and be expelled. The time to achieve a "ready to escape" conformation then limits the kinetics. The scenario is summarized in Figure 8.

The rate-limiting step is thus the transition dynamics between the conformations which have to be much slower for chains under such confinement. This can be understood by considering

that chains under confinement have to obey space-filling criteria, and as long-range fluctuations are strongly damped by the interfacial tension and mutual crossing of the chains are not permitted ("entanglements"), fluctuations are effectively stronger coupled. In other words, the chains have to move more cooperatively, and rearrangement processes are no longer independent processes. This may explain the logarithmical time dependence within the picture of hierarchical constrained dynamics.

To explore the influence of conformational transition dynamics on the exchange kinetics, we are currently undertaking Monte Carlo (MC) simulations of chains under spherical confinement using the bond fluctuation model. By computing the static chain conformation distribution and the number of chains that assume compact conformations close to the interface as a function of MC steps (time), the kinetics according to this scenario can be systematically investigated under different conditions. A detailed presentation of this work and a comparison with the experiments will by presented in a forthcoming paper.

4. Summary and Outlook

In this work a systematic study of the equilibrium chain exchange kinetics between starlike PEP−PEO block copolymers has been presented. Employing a novel time-resolved SANS method, the exchange kinetics of these micelles were studied directly under equilibrium conditions. The results show that the interfacial tension is the key tuning parameter for the chain exchange kinetics. While the kinetics is practically frozen on the accessible time scale in pure water where the interfacial tension is high ($\gamma \approx 46$ mN m^{-1}), the kinetics can be observed after adding moderate amounts of DMF, which lowers γ.

A central observation in this study is that the experimental relaxation curves exhibit a logarithmical decay in time. Such a relaxation behavior is drastically different from what is usually found for ionic low molecular weight surfactant micelles where a single-exponential decay is found with a rate constant of the order of microseconds−milliseconds. Instead, for these polymeric micelles we observe relaxation times of the order of minutes and days and extremely broad distribution evidenced by the logarithmic decay. Similarly, a single-exponential decay is expected from existing theories on polymeric micelles where the process of expulsion is assigned an unique activation energy. Increasing the temperature and decreasing interfacial tension leads to faster kinetics, but the same overall heterogeneous relaxation behavior prevails.

A careful analysis of the kinetical data and the structural properties of the system shows that the apparent broad distribution of expulsion rates cannot be assigned to polydispersity effects or any classical distribution of activation energies. This can be concluded on the basis of the failure to describe the data with a realistic Poisson distribution for the molecular weights or by employing general distribution functions of activation energies, like Gaussian or log−normal distribution, which give rise to unphysical results. Collision-induced chain exchange as was proposed in other works cannot be used as an argument to explain the broad distribution as independent processes would add up individually to the rate constant. Additionally, no concentration dependence on the kinetics was found.

The failure to describe the data assuming parallel independent processes points toward a more complicated picture of the internal dynamics of the micelles than anticipated so far. This is further corroborated by the observed logarithmic relaxation behavior. Such relaxation can be associated with a serial relaxation pattern where the individual steps are closely cor-

related. In this work we propose that such effects are caused by coupling between the internal conformational dynamics of the chains and the expulsion process. So far such effects have been neglected in the discussion of the kinetics of polymeric micelles. Although it is well recognized that the kinetics of polymeric micelles is slower than low molecular weight surfactant micelles, essentially the same mechanism for chain expulsion is assumed. In this work it has been shown that these systems are inherently different and that the topological and geometrical effects characteristic for polymer-like structures are very important for the exchange kinetics.

Employing MC simulations of realistic polymer chains confined to a spherical domain, the structural and dynamical aspects of chains in a micellar core are being studied and compared to the experimental data. These results will be presented in a separate paper.

References and Notes

(1) Aniansson, E. A. G.; Wall, S. N.; Almgren, M.; Hoffmann, H.; Kielmann; Ulbricht, W.; Zana, R.; Lang, J.; Tondre, C. *J. Phys. Chem.* **1976**, *80*, 905.
(2) Wennerström, H.; Lindman, B. *Phys. Rep.* **1979**, *52*, 1.
(3) Hamley, I. W. *The Physics of Block Copolymers*; Oxford University Press: New York, 1998.
(4) Alexandridis, P.; Lindman, B. *Amphiphilic Block Copolymers*; Elsevier: Amsterdam, 2000.
(5) Aniansson, E. A. G.; Wall, S. N. *J. Chem. Phys.* **1974**, *78*, 1024.
(6) Aniansson, E. A. G.; Wall, S. N. *J. Chem. Phys.* **1975**, *79*, 857.
(7) Halperin, A.; Alexander, S. *Macromolecules* **1989**, *22*, 2403.
(8) Dormidontova, E. E. *Macromolecules* **1999**, *32*, 7630.
(9) Waton, G.; Michels, B.; Zana, R. *Macromolecules* **2001**, *34*, 907.
(10) Honda, C.; Abe, Y.; Nose, T. *Macromolecules* **1996**, *29*, 6778.
(11) Willner, L.; Poppe, A.; Allgaier, J.; Monkenbusch, M.; Richter, D. *Europhys. Lett.* **2001**, *55*, 667.
(12) Won, Y. Y.; Davis, T.; Bates, F. S. *Macromolecules* **2003**, *37*, 953.
(13) Wang, Y.; Kausch, C. M.; Chun, M.; Quirk, R. P.; Mattice, W. L. *Macromolecules* **1995**, *28*, 904.
(14) Procházka, K.; Bednár, B.; Mukhtar, E.; Svoboda, P.; Trnená *J. Phys. Chem.* **1991**, *95*, 4563.
(15) Underhill, R. S.; Ding, J.; Birss, V. I.; Liu, G. *Macromolecules* **1997**, *30*, 8298.
(16) van Stam, J.; Creutz, S.; De Schryver, F.; Jérôme, R. *Macromolecules* **2000**, *33*, 6388.
(17) Lund, R.; Willner, L.; Stellbrink, J.; Radulescu, A.; Richter, D. *Macromolecules* **2004**, *37*, 9984.
(18) Daoud, M.; Cotton, J. P. *J. Phys. (Paris)* **1982**, *43*, 531.
(19) Halperin, A. *Macromolecules* **1987**, *20*, 2943.
(20) Stellbrink, J.; Rother, G.; Laurati, M.; Lund, R.; Willner, L.; Richter, D. *J. Phys.: Condens. Matter* **2004**, *16*, S3281.
(21) Laurati, M.; Stellbrink, J.; Lund, R.; Willner, L.; Richter, D. *Phys. Rev. Lett.* **2005**, *94*, 195504.
(22) Likos, C.; Löwen; M. Watzlawek, B.; Abbas, B.; Jucknischke, O.; Allgaier, J.; Richter, D. *Phys. Rev. Lett.* **1998**, *80*, 4450.
(23) Taisne, L.; Walstra, P.; Cabane, B. *J. Colloid Interface Sci.* **1996**, *184*, 378.
(24) Willner, L.; Jucknischke, O.; Richter, D.; Roovers, J.; Zhou, L. L.; Toporovski, P. M.; Fetters, L. J.; Huang, J. S.; Lin, M. Y.; Hadjichristidis, N. *Macromolecules* **1994**, *27*, 3821.
(25) Smith, G. D.; Yoon, D. Y.; Jaffe, R. L.; Colby, R. H.; Krishnamoorti, R.; Fetters, L. J. *Macromolecules* **1996**, *29*, 3462.
(26) Sommer, C.; Pedersen, J. S.; Stein, P. C. *J. Phys. Chem. B* **2004**, *108*, 6242.
(27) Laurati, M. Ph.D. Thesis, University of Münster, 2005.
(28) From the structure factor peak visible in the relevant scattering data at $\phi = 1\%$, we can estimate a mean separation between the micelles, d, of the order of $d = 2\pi/Q^*$, where Q^* is the position of the peak. From the SANS data in Figure 3, we obtain $Q^* \approx 0.0085$ Å^{-1}, which

gives $d \approx 740$ Å. This can be used to estimate the diffusion time between the micelles as $\tau_{\text{diff}} \approx d^2/6D$. Using a typical diffusion constant of $D \approx 1 \times 10^{-11}$ m^2 s^{-1} gives $\tau_{\text{diff}} \approx 90$ μs.

(29) The interfacial tension was in this case strictly measured and compared toward D$_2$O. This is because the densities of d-PEP-OH and H$_2$O are nearly identical, leaving the pendant drop tensiometry method unapplicable. Nevertheless, the interfacial tensions between h-PEP-OH were found to be nearly the same in H$_2$O and D$_2$O.

(30) Richter, D.; Farago, B.; Butera, R.; Fetters, L. J.; Huang, J. S.; Ewen, B. *Macromolecules* **1993**, *26*, 795.

(31) Abramowitz, M.; Stegun, I. A. *Handbook of Mathematical Functions*; Dover Publications Inc.: New York, 1965.

(32) Brey, J. J.; Prados, A. *Phys. Rev. E* **2001**, *63*, 21108.

(33) Tsiok, O. B.; Brazhkhin, V. V.; Lyapin, A. G.; Khvostantsev, L. G. *Phys. Rev. Lett.* **1998**, *80*, 999.

(34) Fernández, A.; Appignasnesi, G. *Phys. Rev. Lett.* **1997**, *78*, 2668.

(35) Persson, B. N. J. *Phys. Rev. B* **1995**, *51*, 13 568.

(36) Brauns, E. B.; Maderas, M. L.; Coleman, R. S.; Murphy, C. J.; Berg, M. A. *Phys. Rev. Lett.* **2002**, *88*, 158101.

(37) Skorobogatiy, M.; Guo, H.; Zuckermann, M. *J. Chem. Phys.* **1998**, *109*, 2528.

(38) Halioğlu, T.; Bahar, I.; Erman, B.; Mattice, W. L. *Macromolecules* **1996**, *29*, 4764.

(39) Palmer, R. G.; Stein, D. L.; Abrahams, E.; Anderson, P. W. *Phys. Rev. Lett.* **1984**, *53*, 958.

(40) Fatkullin, N.; Kimmich, R.; Fischer, E.; Mattea, C.; Beginn, U.; Kroutieva, M. *New J. Phys.* **2004**, *6*, 46.

(41) Lund, R.; Willner, L.; Stellbrink, J.; Lindner, P.; Richter, D. *Phys. Rev. Lett.* **2006**, *96*, 68302.

(42) Fleischer, G.; Rittig, F.; Kärger, J.; Papadakis, C. M.; Mortensen, K.; Almdal, K.; Štépánek, P. *J. Chem. Phys.* **1999**, *111*, 2789.

(43) Rittig, F.; Kärger, J.; Papadakis, C. M.; Fleischer, G. Štépánek, P.; Almdal, K. *Phys. Chem. Chem. Phys.* **1999**, *1*, 3923.

(44) Cavicchi, K. A.; Lodge, T. P. *Macromolecules* **2003**, *36*, 7158.